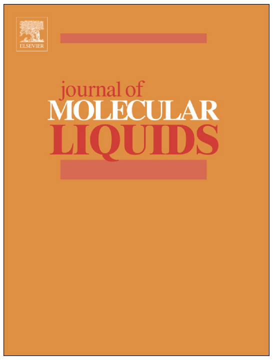

Selective recovery of gold ions in aqueous solutions by a novel trithiocyanuric-Zr based MOFs adsorbent

Zhen Huang, Minghu Zhao, Shixing Wang, Linqing Dai, Libo Zhang, Chen Wang

PII: S0167-7322(19)34631-8

DOI: https://doi.org/10.1016/j.molliq.2019.112090

Reference: MOLLIQ 112090

To appear in: *Journal of Molecular Liquids*

Received date: 18 August 2019

Revised date: 28 September 2019

Accepted date: 7 November 2019

Please cite this article as: Z. Huang, M. Zhao, S. Wang, et al., Selective recovery of gold ions in aqueous solutions by a novel trithiocyanuric-Zr based MOFs adsorbent, *Journal of Molecular Liquids*(2019), https://doi.org/10.1016/j.molliq.2019.112090

Selective recovery of gold ions in aqueous solutions by a novel trithiocyanuric-Zr based MOFs adsorbent

Zhen Huang[a, b, c], Minghu Zhao[a, b, c], Shixing Wang [a, b, c *], Linqing Dai [a, b, c], Libo Zhang [a, b, c], Chen Wang [a, b, c]

[a] State Key Laboratory of Complex Nonferrous Metal Resources Clean Utilization, Kunming University of Science and Technology, Kunming, Yunnan, 650093,PR China

[b] Faculty of Metallurgical and Energy Engineering, Kunming University of Science and Technology, Kunming, Yunnan, 650093, PR China

[c] National Local Joint Laboratory of Engineering Application of Microwave Energy and Equipment Technology, Kunming 650093, China

[*]Corresponding address: Faculty of Metallurgical and Energy Engineering, Kunming University of Science and Technology, Kunming 650093, PR China, Tel.: +86-871-65138997,

[*] E-mail address: wsxkm@sina.com.

Abstract

A trithiocyanuric-Zr based MOFs adsorbent (ZT-MOFs) was synthesized by using trithiocyanuric acid as a linker and zirconium chloride as a metal matrix and used to recover Au(III). ZT-MOFs was characterized by FT-IR, BET, Raman and FE-SEM. ZT-MOFs are porous material and have good stability in the range of pH 1-9. ZT-MOFs showed a higher adsorption capacity for Au(III) (333.34 mg/g) at 480 min and pH=7. The experimental data fitted to Freundlich and pseudo second-order models, indicating a heterogeneous multi-layer chemadsorption is the dominated step.

ZT-MOFs separated selectively Au(III) from laboratory wastewater containing various interfering ions. The removal rate of Au(III) decreased only from 94.5% to 87.5% after 4 adsorption and desorption cycles. This shows that ZT-MOFs have good repeatability. FT-IR, XPS and Zeta potential data shows that the adsorption mechanism of Au(III) on ZT-MOFs is coordination. Therefore, ZT-MOFs have great potential in extracting Au(III) from wastewater.

Keywords: Adsorption, Gold, MOFs, Selectivity

1. Introduction

Gold plays an irreplaceable role in many industrial productions and daily life due to its excellent physicochemical properties, for example, electronic industry, medical devices, aerospace, electronic communications, chemical production and jewelry [1,2]. However, a large amount of gold-containing wastewater is produced in industrial activities, leading to the loss of gold. What's worse, gold is also one of the heavy metal elements and will eventually deposit in the ecosystem when the industrial wastewater is discharged. Gold ions finally enter the food chain and cause serious damage to mankind. So, it is particularly important to recover the available gold ions from industrial wastewater.

The recovering method of gold ions from aqueous solution includes adsorption, solvent extraction, precipitation, ion exchange, and so on [3,4]. Among the recovery methods, adsorption is an emerging recovery method of gold ions in aqueous solution because of its simple operation process, high efficiency and low-cost[5]. The adsorbents can be classified into ion exchange resins, activated carbon, nanocomposite, chitosan, clays, chelating resins and MCM-41[6,8]. As a new type of material adsorbent, metal organic framework (MOFs) has developed rapidly in recent years [9]. Due to high specific surface area, multiple active sites and adjustable pore, MOFs occupied an important position in the many fields, including catalysis[10], drug delivery[11], artificial photosynthesis[9] and removing heavy metal ions[12,13]. Lanthanide metal–organic frameworks was used to adsorb Pb(II) and Cu(II)[14]. The adsorption capacity of nanoporous metal organic framework (MOF-5) for copper ion is 290 mg/g[15]. However, several existing MOFs adsorbents have low selectivity and adsorption capacity because they lack active functional groups, which limits their wide application. Nowadays, many teams attempt to introduce new active functional groups through a post-modification method to improve the adsorption capacity and selectivity of adsorbents. The triol-functionalized Cu-MOF captured selectively mercury species in either the solution or vapor state[16]. Although the post-modification process is effective, it requires extremely expensive reagents and tedious modification processes. Therefore, the introduction of organic functional groups into ligands is a promising method, which can not only simplify the synthesis process, but also improve the selectivity and adsorption capacity.

According to the principle of hard acid and soft acid base (HSAB), sulfur-containing ligands can form stable complexes with Au (III). Trithiocyanuric acid is rich in sulfur atoms and inexpensive. In this study, a new MOFs adsorbent was synthesized by one-step method using trithiocyanuric acid as organic ligand and used to adsorb selectively Au(III) from aqueous solutions. The adsorption effect was evaluated by adjust the pH of the solution, the initial gold ion concentration and the reaction time, etc. The selectivity, repeatability, kinetic and isotherm modes were researched. The adsorption mechanism was also analyzed by X-ray photoelectron spectroscopy(XPS) and X-ray diffraction(XRD).

2 Experimental

2.1 Materials

The gold ion solution were supplied by Nanjing Chemical Reagent Co., Ltd. Hydrochloric acid were supplied by Chengdu Kelon Chemical Reagent Co., Ltd. Trithiocyanuric acid were supplied by Shanghai Aladdin Chemical Co., Ltd. Zirconium tetrachloride were supplied by Shanghai McLean Biochemical Technology Co., Ltd. N,N-dimethylformamide (DMF 99%) were purchased from Shanghai Aladdin Chemical Co., Ltd. HCl (10.0%) and NaOH (10.0%) were used to adjust the pH of the solution.

2.2 Synthesis of adsorbents

A new adsorbent was synthesized by hydrothermal method. Zirconium tetrachloride (2.33g) and Trithiocyanuric acid (1.77g) were weighed according to the molar ratio of 1:1. The mixture was dissolved in solution of 100 mL DMF and 10 mL hydrochloric acid at room temperature. The solution was put into a three-neck reaction bottle and heated to 130℃ for 24 h. After centrifuged, the precipitates were washed five times with DMF and distilled water and dried in vacuum at 70℃ for 24 h. The product was named ZT-MOFs.

2.3. Characterization

Fourier transform infrared spectrum were obtained between 400 cm^{-1} and 4000 cm^{-1} using a Nicolet iS50 spectrophotometer (Thermo Nicolet, USA) with a resolution of 4 cm^{-1}. Inductively coupled optical emission spectroscopy (ICP-OES, Leeman prodigy7, U.S.A) is used to detect ion concentration in solution. Zeta potential was measured at pH 4.0-11.0 using NanoBrook-Omni (Brookhaven Instruments Co., USA). X-ray photoelectron spectroscopy (XPS) was conducted via a PHI-5000 Versaprobe II (Ulvac-Phi, Japan). The surface area of the adsorbent was determined from N_2 adsorption using Micrometitics ASAP 2020 surface area analyzer. The specific surface area was calculated using the Brunauer-Emmett-Teller (BET) method, and the specific pore volume was calculated by the Barrett- Joyner- Halenda (BJH) method. FE-SEM (JSM-7100F, JEOL) was used to detect surface morphology and elemental distribution of samples. Raman Spectra of ZT-MOFs was obtained by JASCO NRS-1000 micro-Raman spectrometer.

2.4. Adsorption experiments

10 mg of the sample was placed in a 15 ml centrifuge tube and 10 ml of a gold ion solution with the concentration at 200 mg/L was added. After mixing, the tube was placed in a ZD-85 gas bath thermostat and shaken for 24 h at 25 ℃ and 300 rpm. After the reaction reached equilibrium, the residual gold ion concentration was measured by ICP-OES. The equation (1) and (2) were used to calculate the adsorption capacity and adsorption rate[17].

$$q_e = \frac{(c_i - c_f)v}{m} \qquad (1)$$

$$R = \frac{C_i - C_f}{C_i} \times 100\% \qquad (2)$$

q_e (mg/g), R (%), C_i (mg/L) and C_f (mg/L) represent the adsorption capacity, the absorption rate, the initial content and the remaining content of gold ion, respectively. V (mL) and m (mg) are the volume of gold ion solution and the weight of ZT-MOFs.

In order to explore the effect of pH on the experiment, ZT-MOFs was added to the gold ion solution with pH from 2 to 11. The different initial concentrations of gold ion solutions(200mg/L-550 mg/L/) were used to study the adsorption isotherms. After mixed ZT-MOFs with gold ion solution, the solution was taken out at set intervals to explore the adsorption kinetics. To investigate the effect of interfering ions, ZT-MOFs was added to a wastewater containing Mg^{2+}, Cr^{2+}, Mn^{4+}, Co^{2+}, Zn^{2+}, As^{3+}, Sb^{2+} and Au^{3+} and waggled for 24 h. After adsorption, the supernatant was detected to obtain the residual ions concentration.

3. Results and Discussion

3.1. Characterization

The surface morphology of ZT-MOFs was observed using FE-SEM (Fig. 1a). It can be observed that the ZT-MOFs adsorbent is formed by stacking many small particles. Fig. 1(b) was the EDS image of area 1 and confirmed the presence of Zr and trithiocyanuric acid. The infrared spectrum of ZT-MOFs is shown in Fig 1(c). The peak at 1589 cm^{-1} indicates that trithiocyanuric acid had an interaction with Zr^{4+}. The peaks at 1589 cm^{-1} and 1715 cm^{-1} are due to the stretching vibration of C-H and C=N[18]. The peaks at 1019 cm^{-1}, 1467 cm^{-1} and 1537 cm^{-1} are due to the stretching vibrations of C=S, CN and NH. The –N-C=S band appeared at 1251 cm^{-1} and 1662 cm^{-1}. Fig 1 (d) is the raman spectrum of ZT-MOFs. The peaks at 143 cm^{-1}, 293 cm^{-1} and 990 cm^{-1} are the characteristic vibration of N-Zr. The characteristic peak at 667 cm^{-1} is caused by the vibration of the C-S bond[19]. So, ZT-MOFs has been successfully synthesized.

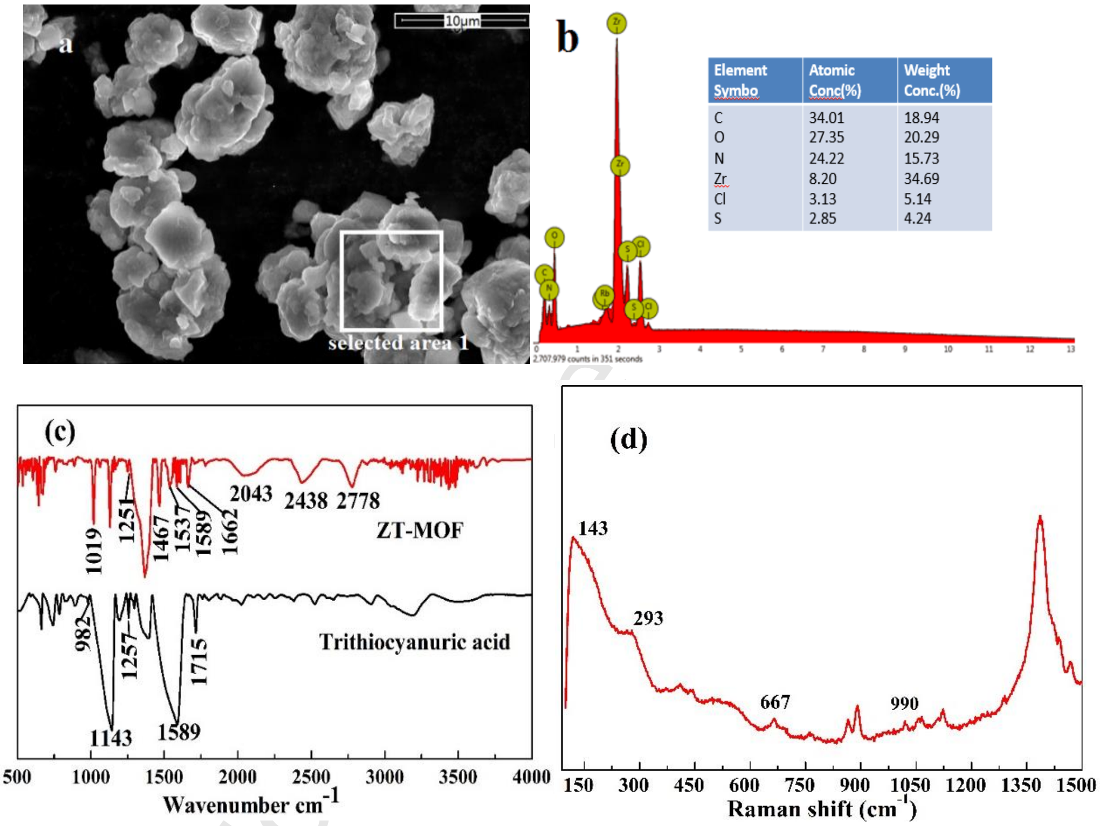

Element Symbo	Atomic Conc(%)	Weight Conc.(%)
C	34.01	18.94
O	27.35	20.29
N	24.22	15.73
Zr	8.20	34.69
Cl	3.13	5.14
S	2.85	4.24

Fig 1. Characterization of ZT-MOFs adsorbent:(a) FE-SEM image (b) EDS image and (c) FT-IR,(d) Raman

To explore the pH stability of ZT-MOFs, Adding of 10 mg ZT-MOFs and 10 ml of water with pH from 1 to 9 in centrifuge tube and shaken for 24 h in a constant temperature. After centrifuged and removed the supernatant, the centrifuge tube was dried to constant weight. The weight of the remaining adsorbent was obtained by subtracting the weight of the centrifugal tube(Fig. 2a). It is found that the weight before and after immersion is unchanged. So, ZT-MOFs have good pH stability.

In order to study the porosity of ZT-MOFs, low temperature N_2 gas adsorption and desorption experiments were carried out on ZT-MOFs (Fig. 2b). The nitrogen adsorption and desorption isotherms of ZT-MOFs show a type IV hysteresis loop, which is a characteristic of mesoporous materials. The average Brunauer-Emmett-Teller (BET) surface area, pore radius and pore volume calculated by the Barrett-Joyner-Halenda (BJH) method were 111.35 m^2/g, 6.88 nm, and 0.102 cm^3/g, respectively. Their high active sites facilitate the rapid mass transfer of Au(III). Au(III) can diffuse into the pores and form a chemical bond with the inner surface of the mesopores.

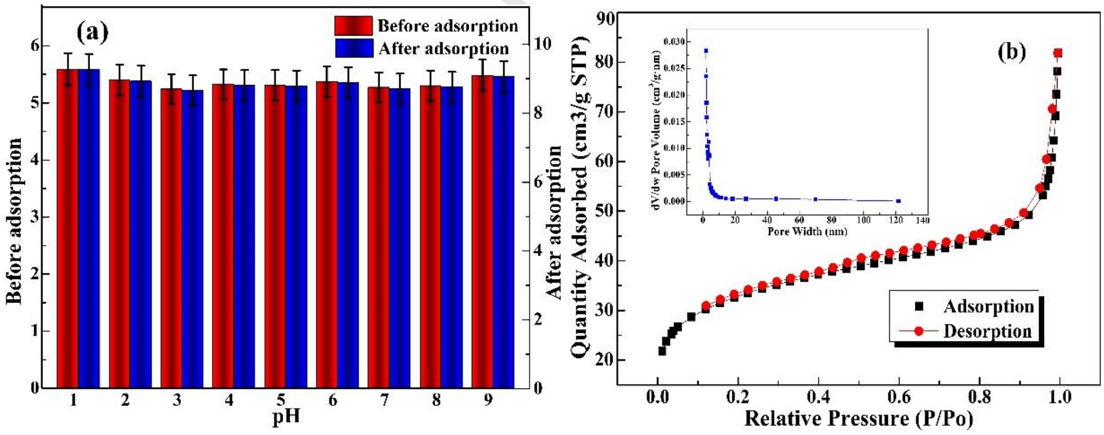

Fig.2 (a) pH stability and (b) BET of ZT-MOFs

3.2. Effect of pH on removal rate and zeta potential

In the adsorption process, pH has a crucial effect on the adsorption capacity .The highest adsorption capacity of ZT-MOFs for Au(III) is obtained at neutral and weak base conditions (Fig. 3a). When the pH increases from 2 to 7, the removal rate increase and finally reach the maximum. When pH is 7.0, the maximum removal rate is 93%. At lower pH, the concentration of hydrogen ion is higher, and a large number of free hydrogen ions exist in the solution. These free hydrogen ions will compete adsorption points with chloroauric acid ions on the adsorbent surface. Therefore, the removal rate of Au(III) decreased with the decrease of pH. When the pH is higher than 7, complexes such as $AuCl_3(OH)^-$, $AuCl_2(OH)^{2-}$ $AuCl(OH)^{3-}$, and $AuCl(OH)^-_4$ are produced. So the removal rate is remarkably lowered. The optimum pH is 7.0.

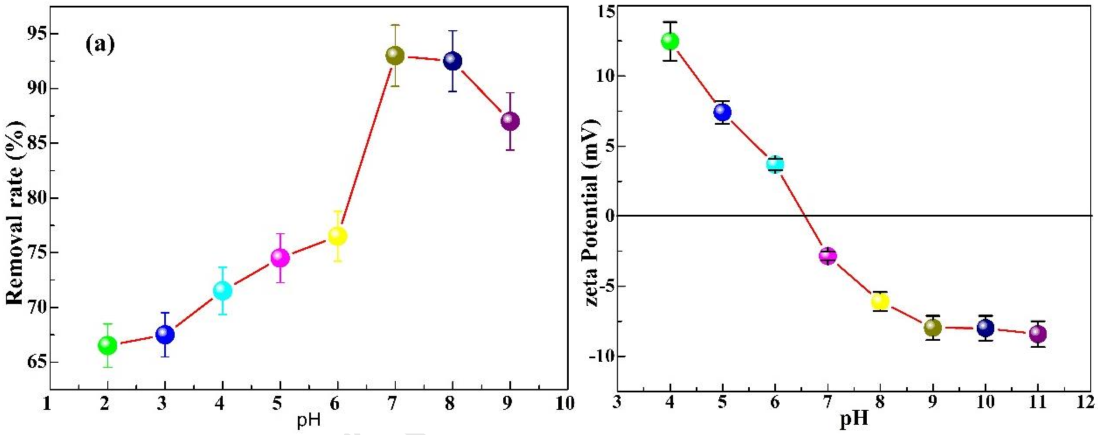

Fig.3 (a) The effects of pH value on the adsorption of Au(III) and (b) zeta potential of ZT-MOFs

Fig. 3(b) is the zeta potential of ZT-MOFs. The isoelectric point of ZT-MOFs is 6.4. When the pH is less than 6.4, ZT-MOFs has a positive charge. Conversely, when the pH is greater than 6.4, ZT-MOFs has a negative charge. The literature indicates that Au(III) species are mainly present as negative charges in acidic solutions (pH from 2 to 6). There was no significant correlation between adsorption rate and Zeta potential, indicating that the adsorption mechanism of ZT-MOFs is not ion exchange and electrostatic interaction.

3.3. The effect of initial Au(III) concentration and adsorption isotherms

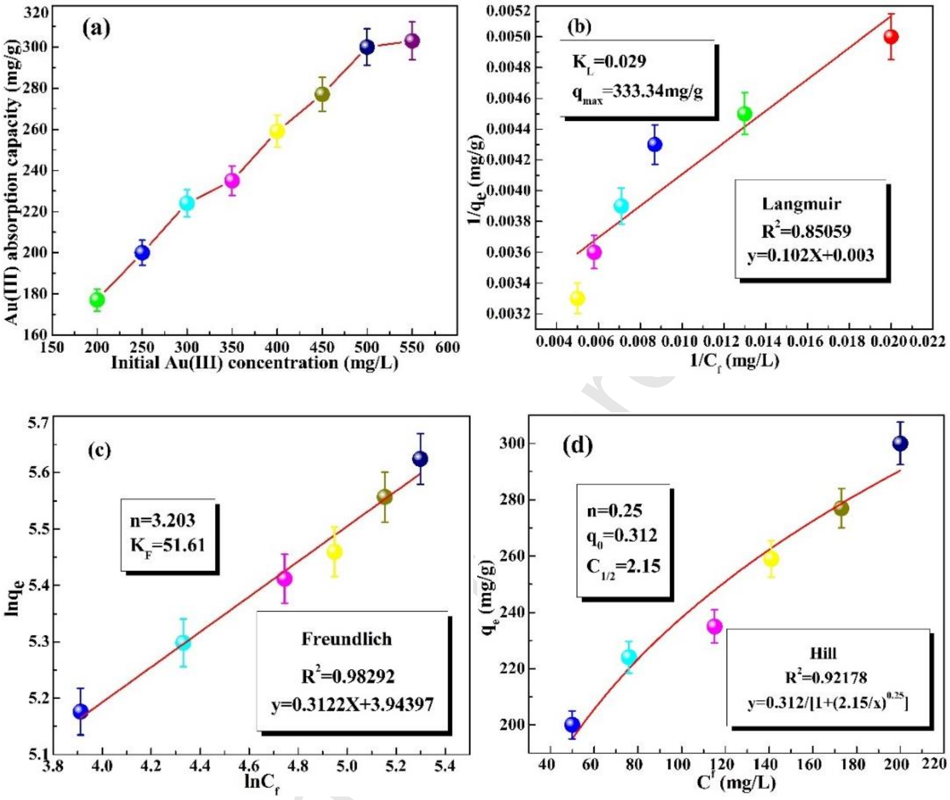

Fig.4 Effect of the initial Au(III) concentration on gold adsorption. The linearized isotherm models for gold adsorption on ZT-MOFs:

Langmuir(b), Freundlich(c) and Hill(d)

Adsorption capacity is an important factor to understand how many adsorbents are necessary for valid enrichment of adsorbates in a given solution. To evaluate the adsorption capacity of ZT-MOFs, the effect of the initial Au(III) concentration was investigated (Fig.4a). With the increase of initial Au (III) concentration, the adsorption capacity of ZT-MOFs for Au (III) increases rapidly. When the initial concentration of Au (III) reached 550 mg/L, the adsorption reached its maximum. At low concentrations, the surface binding site of the adsorbent can fully bind to Au(III). However, as the concentration of Au(III) increases, the adsorption site on the surface of the adsorbent reaches saturation and gold ions can no longer be adsorbed. The maximum adsorption capacity of gold ion on ZT-MOFs is 333.34 mg/g. Table 1 lists some Au(III) adsorbents. It can be found that the maximum adsorption capacity of ZT-MOFs was higher than that of other adsorbents. In general, ZT-MOFs was a very effective adsorbent for Au(III).

Table 1 Comparison of the Au(III) adsorbing capacity of ZT-MOF and adsorbent reported in the references

Adsorbent	**Adsorption capacity (mg/g)**	**pH**	**Time (h)**	**Cycles**	**References**
aminopropyltriethoxysilane-functionalized lignocellulosic coconut pith	261.36	4	2	3	[20]
P(Penta3MP4/PEG-DA/HEMA）	45.19	0.5	2	3	[21]
Tetraalkyl phosphonium chloride	140	1	2	4	[22]
2,2-dimethoxy-2-phenylacetophenon	118.81	5	5	4	[23]
$Fe_3O_4@SiO_2$-SH	84.75	5	4	5	[24]
Aliquat-336-impregnated alginate capsule	191.92	1	2	4	[25]
nanosilica with guanidinium ionic liquids	120.56	5	2.5	5	[26]
ZT-MOF	333.34	7	8	4	This work

In this study, adsorption isotherms can be used to obtain some important data and to understand the adsorption process. The Langmuir, Freundlich and Hill isotherm models were used to fit the experimental data. Langmuir is used for single-layer adsorption and can be described as the dynamic equilibrium between adsorption and desorption of single layer phase points on the surface of the adsorbent(Eq3). The Freundlich model was used for multilayer adsorption. It is described that the adsorption of multiple layers at different phase points is different(Eq 4). The Hill model is used for adsorption of different adsorbed species on the surface of the adsorbent. It can be used to describe the synergy between a single ligand and different phase points on the same surface (Eq 5). The isothermal adsorption models are described as the following equations:

$$\frac{1}{q_e} = \frac{1}{q_m} + \frac{1}{K_L q_m} . \frac{1}{C_f} \qquad (3)$$

$$\ln q_e = lnK_F + \frac{1}{n} lnC_f \qquad (4)$$

$$q_e = \frac{nN_m}{1+\left(\frac{C_{1/2}}{C_f}\right)^n} \qquad (5)$$

In the above formula, C_f(mg/L), q_e(mg/g) and q_m(mg/g) are equilibrium concentrations, equilibrium adsorption capacity and maximum adsorption capacity. K_L, K_F, K_G are the constants of Langmuir, Freundlich and Hill models, n is the number of metal ions on per site, N_m(mg/g) represents the density of the receptor site, $C_{1/2}$ (mg/L) and C_e (mg/L) represent the concentration at half equilibrium and saturation.

Table2 Isotherm parameters of Au(III) adsorption

Isotherm models	**Parameters**	**Valu**
Langmuir	q_{max}	333.34
	K_L	0.029
	R^2	0.851
Freundlich	K_F	51.61
	n	3.203
	R	0.983
Hill	q_0	0.312
	$C_{1/2}$	2.15
	n	0.25
	R^2	0.921

Fig 3 (b-d) is a linear fit of the three isotherm models, and the fit data is shown in Table 2. It can be seen from the figure that the order of the fitting coefficient R^2 of the three isothermal models is $R^2_{Freundlich}> R^2_{Hill}> R^2_{Langmuir}$. From the point of view of the fitting coefficient, the Freundlich model is more in line with the adsorption process. This indicates that the adsorption process of Au(III) in ZT-MOFs is a heterogeneous multi-layer adsorption process. Because its binding sites are unevenly distributed on the ZT-MOFs. For K_F, the magnitude of the n value indicates the adsorption capacity of the adsorbent for Au(III). In general, the larger the value of K_F, the greater the adsorption capacity of the adsorbent for Au(III). For the value of n, when $1 < n < 10$, it is advantageous for the occurrence of the adsorption process. The larger the value of n, the stronger the adsorption capacity. In Table 2, n=3.203. It indicates that ZT-MOFs has strong adsorption capacity for Au(III).

3.4. Effect of adsorbing time and adsorption kinetics

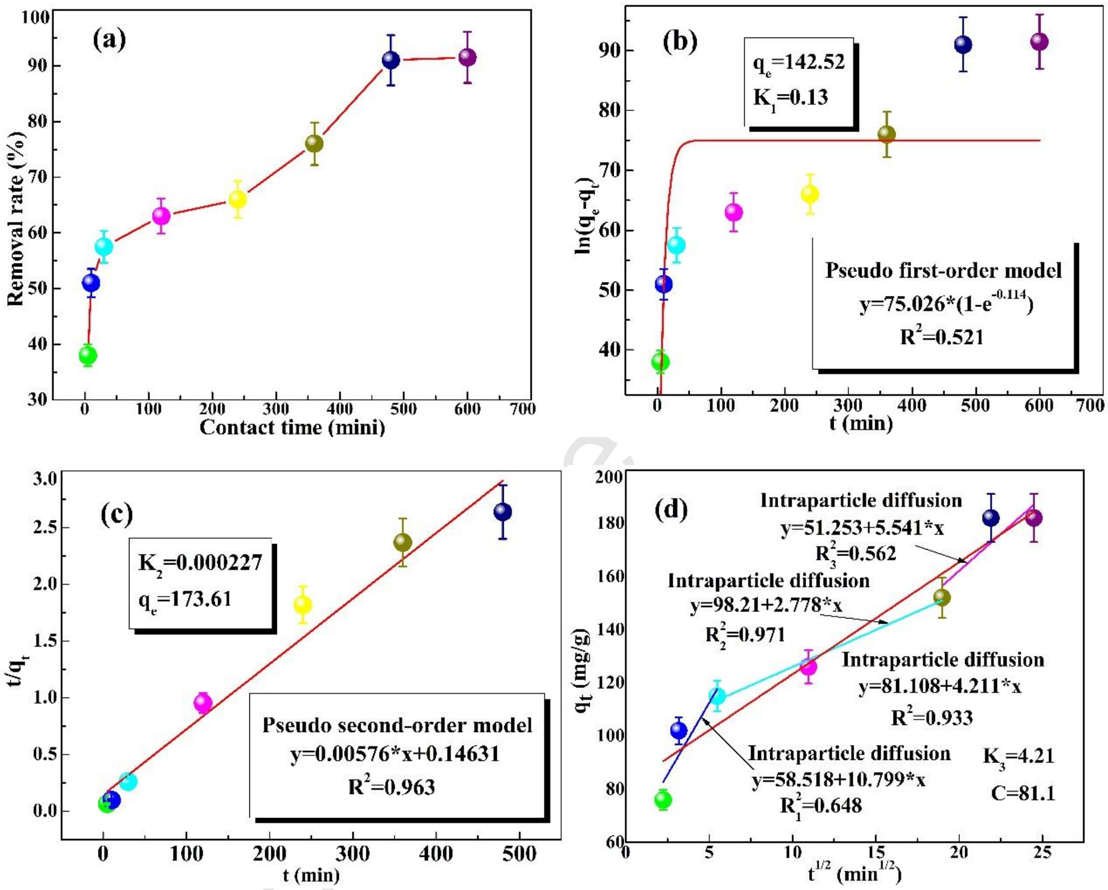

Fig.5 Effect of absorbing time (a). Linearized kinetics model for gold adsorption on ZT-MOFs: (b) pseudo-first-order model,(c) pseudo-second-order model and (d)intraparticle diffusion model

The adsorption speed is one of the important factors to evaluate the adsorbent properties. Fig. 5(a) shows the effect of time change on the adsorption rate. As shown in Fig. 5(a), it can be seen that the adsorption process is divided into three stages. In the first 60 min, the adsorption rate is very fast. The removal rate reached 57% due to the rich adsorption sites on the surface of the adsorbent in the initial stage. In the period of 60 to 480 minutes, the adsorption rate also increases gradually with time and the removal rate only reaches 91%. Because the active site on the surface of the adsorbent is covered. The adsorption process of Au(III) by ZT-MOFs reaches equilibrium in about 480 min, and the maximum adsorption amount reach 182 mg/g at pH=7.0. It is usually necessary for most reported sewage treatment materials to reach equilibrium in a few days. Thus, it can be seen that the ZT-MOFs adsorbent has the advantage of rapidly removing gold ions and is also superior to other adsorbent materials.

For the above dynamics part, pseudo-first-order dynamics model (6), pseudo-second-order dynamic model (7) and intra-particle diffusion model (8) can be used for data analysis. The model can be expressed by the following formulas

$$q_t = q_e(1 - \mathrm{e}^{-K_1 \mathrm{t}}) \tag{6}$$

$$\frac{t}{q_t} = \frac{1}{K_2 q_e^2} + \frac{t}{q_e} \tag{7}$$

$$q_t = K_3 t^{\frac{1}{2}} + C \tag{8}$$

In the above formula, q_e(mg/g), q_t(mg/g) and t(min) are the adsorption capacity at equilibrium time, the adsorption capacity at any time and the adsorption time. Among them, K_1, K_2 and K_3 are the invariant parameters of the three adsorption kinetic models. The linear fit of the data is shown in Fig. 4(b-d)

Table 3 The parameters of the kinetics models

Kinetics model	Parameters	Values
Pseudo-first-order	K_1	0.13
	R^2	0.52122
	q_e	142.52
Pseudo-second-order	K_2	0.000227
	R^2	0.96
	q_e	173.61
Intraparticle diffusion	K_3	4.21
	R^2	0.93253
	C	81.1

The pore diffusion rate is a control step in the pseudo first order model. The adsorption rate control step is chemisorption in a pseudo-secondary model. Intraparticle diffusion models include porous diffusion and surface diffusion. Fig.5 (b-d) are linear fit data for the three models, and Table 3 gives data for the three models. The order of the linear fitting coefficient (R^2) in the three models is the pseudo second order (0.96) intraparticle diffusion (0.93) pseudo first order (0.52). The calculated second-order model equilibrium adsorption amount (q_e) is about 172 mg / g, which is larger than the pseudo first-order model. It can be inferred that the adsorption process of Au(III) by ZT-MOFs is more in line with the pseudo second-order kinetic model. It is indicated that the adsorption process of Au(III) by ZT-MOFs is chemical adsorption. The intraparticle diffusion process is divided into three steps: mass transfer, adsorption and diffusion. As shown in Fig5 (d). Step (I) is dominated by the process of external mass, so the diffusion within the particles is faster, so that the mass transfer process is completed in a short time. Step (II) is the adsorption process of Au(III) on the surface of ZT-MOFs. Therefore, adsorption and diffusion are the main control steps. As the binding site of the ZT-MOFs surface gradually decreases, the adsorption rate becomes slow and eventually reaches equilibrium in step (III). Combined with the data, it can be judged that the adsorption restriction step of ZT-MOFs on Au(III) is chemical adsorption.

3.5 Reusability and practicality of ZT-MOFs

Repeatability is an important property of adsorbents. 50 mg of ZT-MOFs was placed in a 100 ml centrifuge tube, 50 ml of a gold ion solution having a concentration of 200 ppm also was added. The mixture was shaken at 25 ℃ for 24 h in a constant temperature shaking box. The supernatant was acquired by centrifugal separation, and the remaining Au(III) concentration was measured. The residual solid was added to 10% pure thiourea(50 ml) and placed in a constant temperature shaking box and shaken at 25 ℃ for 24 h. After centrifuged and washed five times with distilled water. The second adsorption test was carried out. This process was repeated 4 times. The adsorption amount and removal rate of Au(III) are shown in Fig. 6(a). It can be seen from the data that the removal rate of the four repeated adsorption and desorption Au(III) is only decreased by 7%. Table 1 lists also the regeneration times of adsorbent reported in the literatures. The regeneration times of ZT-MOFs is higher than these of adsorbent reported in the literatures. Therefore, the use of this adsorbent can significantly reduce the cost due to its higher adsorption capacity and more renewable cycles.

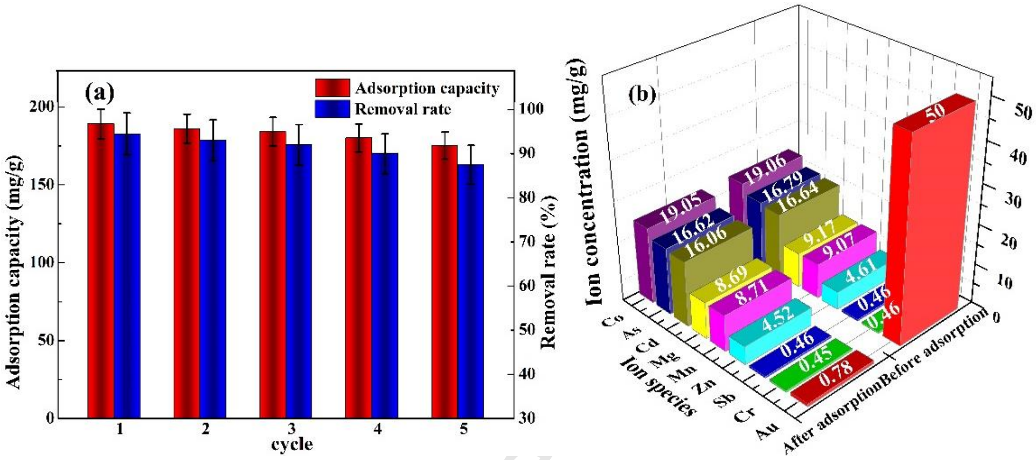

Fig.6 Practicality(a) and Repeatability(b)and of the ZT-MOFs

In order to evaluate the practicality of ZT-MOFs and better use it in industrial production, wastewater from laboratories was used. First, the pH of the wastewater was adjusted to 7.0 and ICP-OES is used to determine the type and amount of metal ions in the wastewater. Then, 10 mg of ZT-MOFs was added to 10 ml of wastewater. The mixture was placed in a constant temperature shaking box and shaken at 25 ℃ for 24 h. The mixture was separated by centrifugation and the type and content of the metal ions in the supernatant liquid were measured by ICP-OES. The data is shown in Fig 6(b). It can be seen that ZT-MOFs hardly adsorbs other kinds of metal ions. At the same time, ZT-MOFs has an extremely high selectivity for Au(III).

The affinity and selectivity of ZT-MOFs for Au(III) was investigated by using the partition coefficient (K_{dc}) and the selectivity coefficient (k). When the value of

K_{dc} is large, it indicates that ZT-MOFs can remove Au(III) well. Conversely, when the value of K_{dc} is small, it indicates that a large amount of Au(III) is still present in the solution. The values of K_{dc} and K obey Eq(9) and (10).[28,29]

$$K_{dc} = \frac{q_e}{C_f} \qquad (9)$$

$$\mathrm{k} = \frac{K_{dc}(A_u)}{K_{dc}(M_i)} \qquad (10)$$

Where C_f(mg/L) represents the remaining concentration; K_{dc}(Au) represents the distribution coefficient of Au(III), and K_{dc}(Mi) represents the distribution coefficient of other ions.

Table 4 Adsorption results of ZT-MOFs in practical application.

Metal ions	C_0 (mg/L)	C_f (mg/L)	q_e (mg/g)	R (%)	K_{dc} (L/g)	K
Au	50	0.78	49.22	0.9844	63.103	-
Cr	0.46	0.45	0.01	0.0217	0.0222	2842.478
Sb	0.46	0.46	0	0	0	-
Zn	4.61	4.52	0.09	0.0195	0.0199	31711
Mn	9.07	8.71	0.36	0.0397	0.0413	1527.919
Mg	9.17	8.69	0.48	0.0523	0.0553	1143.177
Cd	16.34	16.06	0.28	0.0171	0.0174	3626.610
As	16.79	16.62	0.17	0.0101	0.0102	6186.570
Co	19.06	19.05	0.01	0.0005	0.00053	120196.29

It can be seen from Table 4 that the K_{dc} value of Au(III) far exceeds that of the interfering ions, and thus it can be proved that ZT-MOFs has the highest affinity for Au(III). It can be seen that the K value of Au(III) is larger than that of the interfering ions, which indicates that the interfering ions in the wastewater are easily substituted by Au(III). Au(III) is in the soft metal ion and has a large affinity with the sulfur group. This shows that ZT-MOFs has great potential in practical applications.

3.6 Adsorption mechanism

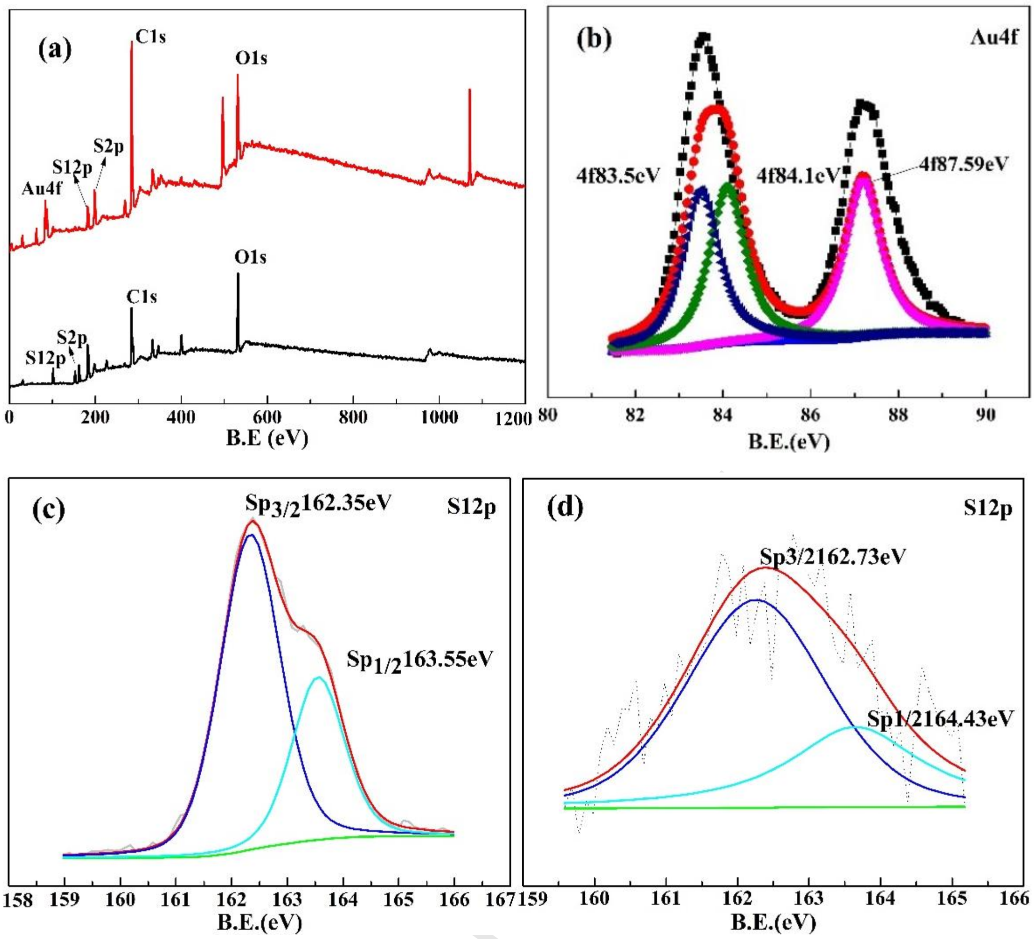

Fig. 7. XPS spectra of ZT-MOFs, ZT-MOFs-Au (a); Au4f spectra of ZT-MOFs-Au (b); S 2p spectra of ZT-MOFs before adsorption (c) and after adsorption (d).

Fig. 7 shows the spectrum of XPS of ZT-MOFs and ZT-MOFs-Au. The peak of Au can be clearly observed in Fig.7 (a). The peak corresponds to Au4f in Fig 7 (b), indicating that Au(III) is absorbed by the ZT-MOFs adsorbent. It can be seen from Fig 7 (b) that the peaks at 84.36 eV (Au $4f_{7/2}$) and 87.36 (Au $4f_{5/2}$) corresponded to Au (III)[30,31]. Because there is no absorption peak of Au^0 in the figure, it can be determined that the adsorption mechanism of ZT-MOFs is a coordinated interaction. Fig. 5(c) is a high-resolution spectrum of $Sp_{1/2}$ and $Sp_{3/2}$ before ZT-MOFs adsorbs

Au(III). The binding energy was 162.35 eV for $Sp_{3/2}$ and 163.55 eV for $Sp_{1/2}$. In Fig. 7(d), the peak value of $Sp_{1/2}$ becomes 162.73 eV and 164.43 eV[32,33]. The increase of binding energy is attributed to the interaction between ZT-MOFs and Au(III). Therefore, it can be explained that S is related to Au(III) when ZT-MOFs adsorbs Au(III).

4. Conclusions

A trithiocyanuric-Zr based MOFs adsorbent was successfully synthesized for recovering Au(III) from solution. The synthesis of ZT-MOFs can be proved by FT-IR and Raman spectra. ZT-MOFs are porous material with higher specific surface area. ZT-MOFs is stabile in the range of pH from 1 to 9. ZT-MOFs can effectively adsorb Au(III) from solution at pH 7. The maximal adsorption capacity of Au(III) on ZT-MOFs is 333.34 mg/g. The adsorption process followed the pseudo-second-order kinetics and Freundlich isotherm models, indicating the adsorption of Au(III) was a heterogeneous multi-layer chemadsorption. ZT-MOFs can be regenerated at least 4 cycles, and the adsorption capacity slightly decreased with the increase of the regenerated cycles. ZT-MOFs selectively adsorbed Au(III) from wastewater. The adsorption effect comes from coordination between Au(III) and the function groups of ZT-MOFs. The present work indicate that ZT-MOFs is very promising for the extraction of Au(III) from wastewater.

Acknowledgments

The authors are grateful to the National Natural Science Foundation of China Project (Nos. U1702252 and 51664037).

References

[1] P. P. Prof, Theoretical chemistry of gold, Chem. Int. Ed. 43 (34) (2004)4412–4456.

[2] C.W. Corti, R.J. Holliday, Commercial aspects of gold applications: frommaterials science to chemical science, Gold Bull. 37 (1) (2004) 20–26.

[3] M. Gurung, B. Babu Adhikari, H. Kawakita, K. Ohto, K. Inoue, S. Alam, Recovery of Au(III) by using low cost adsorbent prepared from persimmon tannin extract, Chem Eng J. 174 (2011) 556– 563.

[4] N. Saman, M. U. Rashid, J. W. P. Lye, H. Mat, Recovery of Au(III) from an aqueous solution by aminopropyltriethoxysilane-functionalized lignocellulosic based adsorbents, React Funt Polym,123(2018)106-114.

[5] G. Lin, S. X. Wang, L. B. Zhang, T. Hu, S. Cheng, L. K. Fu, C. Xiong, Enhanced and selective adsorption of Hg^{2+} to a trace level using trithiocyanuric acid-functionalized corn bract, Environ Pollut, xxx (2018) xxx-xxx. doi.org/10.1016/j.envpol.2018.08.054

[6] M. R,, Awual. Novel nanocomposite materials for efficient and selective mercury ions capturing from wastewater, Chem Eng J. 307(2017), 456-465.

[7] N. Li ,R. Bai, C. k. Liu, Enhanced and Selective Adsorption of Mercury Ions on Chitosan Beads Grafted with Polyacrylamide via Surface-Initiated Atom Transfer Radical Polymerization, Langmuir.21(2005), 11780-11787. doi:10.1021/la051551b

[8] D. Xu, W. D. Wu, H-J. Qi, R-X. Yang, W-Q Deng, Sulfur rich microporous polymer enables rapid and efficient removal of mercury(II) from water, Chemosphere.196(2018),174-181.

[9] Y-Z. Chen, R. Zhang, L. Jiao, H-L. Jiang, Metal–organic framework-derived porous materials for catalysis, Coordin Chem Rev. 362 (2018) 1–23.

[10] Q. Xia, Z. Li, C. Tan, Y. Liu, W. Gong, Y. Cui, Multivariate Metal–Organic Frameworks as Multifunctional Heterogeneous Asymmetric Catalysts for Sequential Reactions, J Am Chem Soc, 139 (2017) 8259–8266.

[11] J. Zhuang, C-H. Kuo, L-Y. Chou, D-Y. Liu, E. Weerapana, C-K. Tsung, Optimized Metal–Organic-Framework Nanospheres for Drug Delivery: Evaluation of Small-Molecule Encapsulation, ACS Nano, 8 (2014) 2812–2819.

[12] J. Y. Lee, O. K. Farha, J. Roberts, K. A. Scheidt, S. B. T. Nguyena, J. T. Hupp, Metal–organic framework materials as catalysts, Chem Soc Rev, 38 (2009) 1450–1459.

[13] N. A. Khan, Z. Hasan, S. H. Jhung, Adsorptive removal of hazardous materials using metal-organic frameworks (MOFs): A review, Hazard Mater, 244 (2013)444–456.

[14] A. Jamali, A. Tehrani, F. Shemirani, & A. Morsali, Lanthanide metal–organic frameworks as selective microporous materials for adsorption of heavy metal ions. Dalon T. 45(2016) 9193-9200.

[15] N. Bakhtiari，S. Azizian，Adsorption of copper ion from aqueous solution by nanoporous MOF-5: A kinetic and equilibrium study，J Mil Liq, 206(2015) 114-118.

[16] W. Xu, S. He, S. Liu, X. Liu, Y. Qiu, W. Liu, X. Liu, L. Jiang, J. Jiang, Post-synthetic modification of a metal-organic framework based on 5-aminoisophthalic acid for mercury sorption, Inorg Chem Commun, 108 (2019) 107515.

[17] G. Lin, S. X. Wang, L. B. Zhang, T. Hu, J. H. Peng, S. Cheng, L. K. Fu, Synthesis and evaluation of thiosemicarbazide functionalized corn bract for selective and efficient adsorption of Au(III) from aqueous solutions, J Mol Liq, 258 (2018) 235–243.

[18] W. S. Liu, K. L. Koh, J. l. Lu, L.P. Yang, S. L. Phua, J. H. Kong, Z. Chena, X. H.Lu, Simultaneous catalyzing and reinforcing effects of imidazole-functionalized graphene in anhydride-cured epoxies, J Mater Chem, 22(2012)18395-18402.

[19] R. Ullah , X. Wang, Raman spectroscopy of Bisphenol ‘S’ and its analogy with Bisphenol ‘A’ uncovered with a dimensionality reduction technique, J Mol Struct, 1175 (2019) 927-934.

[20] N. Saman, M. Rashid, J. Lye, H. Mat, Recovery of Au(III) from an aqueous solution by aminopropyltriethoxysilane-functionalized lignocellulosic based adsorbents, React Funct Polym, 123 (2018) 106–114.

[21] M. Fırlak, M. Kahraman, E. Yetimoğlu, Preparation and Characterization of Photocured Thiol-Ene Hydrogel: Adsorption of Au(III) Ions from Aqueous Solutions. J Appl Polym Sci, 126(2012)0-0.

[22] K. Campos, T. Vincent, P. Bunio, A. Trochimczuk, E. Guibal, Gold Recovery from HCl Solutions using Cyphos IL-101 (a Quaternary Phosphonium Ionic Liquid) Immobilized in Biopolymer Capsules, Solvent Extr Ion Exc, 26(2008)570-601.

[23] M. Fırlak, E. Yetimoğlu, M. Kahraman, Adsorption of Au(III) ions from aqueous solutions by thiol-ene photoclick hydrogels and its application to electronic waste and geothermal water, J Water Process Eng, 3 (2014) 105–116.

[24] Y. Zhang, Q. Xu, S. Zhang, J. Liu, J. Zhou, H. Xu, H. Xiao, J. Li, Preparation of thiol-modified Fe3O4@SiO2 nanoparticles and their application for gold recovery from dilute solution, Sep Purif Technol, 116 (2013) 391–397.

[25] W. Wei, D. Reddy, J. Bediako, Y. Yun, Aliquat-336-impregnated alginate capsule as a green sorbent for selective recovery of gold from metal mixtures, Chem Eng J, 289 (2016) 413–422.

[26] C. Xiong, Y. Li, S. Wang, Y. Zhou, Functionalization of nanosilica via guanidinium ionic liquid for the recovery of gold ions from aqueous solutions, J Mol Liq, 256 (2018) 183–190.

[27] C. Xiong, S. Wang, L. Zhang, Y. Li, Y. Zhou, J. H. Peng, Selective recovery of silver from aqueous solutions by poly (glycidyl methacrylate) microsphere modified with trithiocyanuric acid, J Mol Liq,254(2018)340-348.

[28] M. Tanzifi, S. Hosseini, A. Kiadehi, M. Olazar, K. Karimipour, R. Rezaiemeh, I. Ali, Artificial neural network optimization for methyl orange adsorption onto polyaniline nano-adsorbent: Kinetic, isotherm and thermodynamic studies, J Mol Liq,244(2017)189-200.

[29] C. Xiong, S. Wang, L. Zhang, Selective recovery mechanism of Au(III) from an aqueous solution by trimethyl phosphate modified poly(glycidyl methacrylate), J Taiwan Inst Chem E, 000(2018)1–10.

[30] X. Wang, Y. Zheng, A. Wang, Fast removal of copper ions from aqueous solution by chitosan-g-poly(acrylic acid)/attapulgite composites, J Hazard Mater,169(2009)970-977.

[31] X. Wang, L. Yang, J. Zhang, C. Wang, Q, Li, Preparation and characterization of chitosan–poly(vinyl alcohol)/bentonite nanocomposites for adsorption of Hg(II) ions, Chem Eng J,251(2014)404-412.

[32] X. Li, C. Zhang, R. Zhao, X. Lu, X. Xu, X. Jia, C. Wang, L. Li, Efficient adsorption of gold ions from aqueous systems with thioamide-group chelating nanofiber membranes, Chem Eng J,229(2013)420-428.

Conflicts of Interest

The authors declare no conflict of interest.

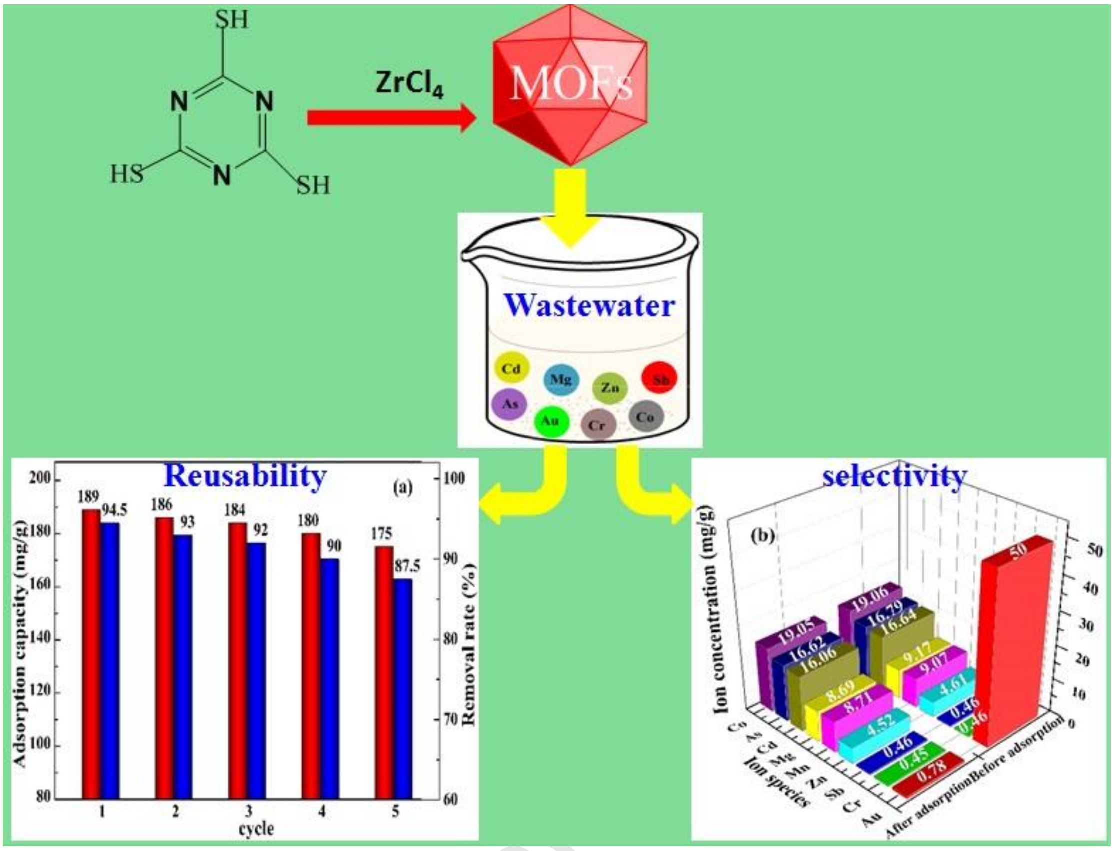

Graphical abstract

Highlights

1. A novel Zr-based MOFs adsorbents was prepared by one-step method.
2. Adsorbent shows good reusability and selectivity for Au(III).
3. Adsorption mechanism was chelation.
4. Adsorbent separated successfully Au(III) from the laboratory wastewater.